

# Charm production at HERA

G.P. Heath<sup>a\*</sup>

<sup>a</sup>H.H. Wills Physics Laboratory, University of Bristol, Bristol BS8 1TL, UK

## 1. INTRODUCTION

The HERA collider circulates beams of electrons (positrons) and protons at energies of 27.5 and 820 GeV respectively. The  $e^\pm p$  centre of mass energy for collisions between the beams is 300 GeV. The largest cross-section processes observed in these collisions are photoproduction reactions, where the  $e^\pm$  beam acts as a source of almost real ( $Q^2 \ll 1 \text{ GeV}^2$ ) photons. Processes where a virtual photon of sizeable  $Q^2$  is exchanged are known as Deep Inelastic Scattering, or DIS reactions. In this paper I review measurements of open charm production at HERA made in both photoproduction and DIS by the H1 and ZEUS collaborations.

Charm quarks are produced in real or virtual photon–proton collisions predominantly via the photon–gluon fusion process illustrated in Figure 1a. Charm production is therefore sensitive to the gluon momentum distribution in the proton. Other contributing processes are also shown in Figure 1. The diagram of Figure 1b, where the charm quark is an active constituent of the proton, is expected to be important in DIS at large  $Q^2$ . In photoproduction, additional contributions may arise from “resolved photon” processes as shown in Figure 1c, which reveal the partonic structure of the photon. Sources of charm production other than via the hard processes shown, such as fragmentation or the decay of  $b$  quarks, are negligible by comparison.

Cross-section calculations for these processes in the framework of perturbative QCD should be reliable, since the relatively large charm quark mass  $m_c > \Lambda_{QCD}$  provides a hard scale in all cases. In addition, in many kinematic regions, further hard scales are provided by a large photon virtuality  $Q^2$  or high transverse momentum of the produced charm quark pair. A number of authors have produced calculations of charm production to next-to-leading order (NLO) in QCD.

The analyses reviewed here are based on data taken in 1994, when each experiment collected around  $3 \text{ pb}^{-1}$  of positron–proton collisions. Both H1 and ZEUS reconstruct charm signals using the invariant masses of tracks found in the tracking detectors. No particle identification is used. I cover only the production of open charm;  $c\bar{c}$  meson signals are discussed in the contribution to this conference on vector mesons at HERA[1].

Throughout this paper I use standard symbols for event-related kinematic quantities at HERA.  $Q^2$  is the invariant squared 4-momentum transfer

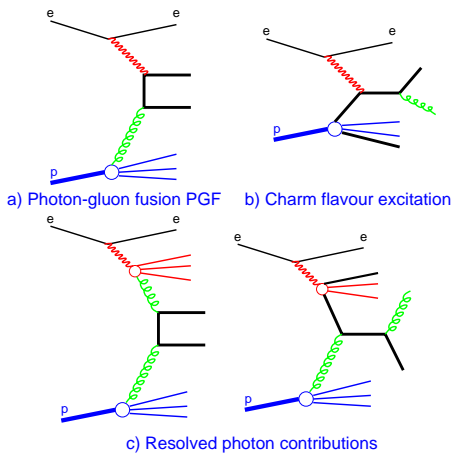


Figure 1. Charm production processes at HERA.

\*on behalf of the ZEUS and H1 collaborations.

from the positron to the hadronic system, written as a positive quantity;  $Q^2 = -q^2 = -(k - k')^2$ , where  $k, k'$  are the initial and final state positron 4-momenta. The Bjorken scaling variable  $x$  is defined by  $x = \frac{Q^2}{2p \cdot q}$ , where  $p$  is the initial proton beam 4-momentum.  $x$  is the fractional momentum carried by the struck parton, in the parton model of DIS processes.  $W$  is the invariant mass of the final state hadron system, or the  $\gamma^*p$  invariant mass given by  $W^2 = (p + q)^2$ . These three quantities are related by  $Q^2 = W^2 \left(\frac{1-x}{x}\right)$ . Finally, the variable  $y = \frac{p \cdot q}{p \cdot k} = \frac{Q^2}{xs}$  where  $\sqrt{s}$  is the total  $ep$  centre-of-mass energy.

This review is divided into two main sections, and a short summary. In section 2 I discuss charm photoproduction measurements and QCD calculations. Charm production in DIS, and measurements of the charm contribution to the proton structure function, are presented in section 3.

## 2. OPEN CHARM IN PHOTOPRODUCTION

The techniques used by the two collaborations[2,3] to reconstruct charm candidates in photoproduction events are similar. The aim is to identify the decay chain

$$D^*(2010)^+ \longrightarrow D^0 \pi_s^+ \longrightarrow K^- (n\pi)^+ \pi_s^+ \quad (1)$$

and its charge conjugate, where  $\pi_s^+$  is a ‘‘slow’’ pion carrying only 40 MeV of momentum in the  $D^{*+}$  rest frame. The analysis uses pairs of oppositely charged tracks to search for  $D^0$  candidates, and ZEUS also has a signal from 4-track combinations. Each track in turn is assigned the charged kaon mass, with the remainder assumed to be pions. Combinations whose invariant mass  $m_{K\pi}$  falls within a window around the  $D^0$  mass are then further combined with a track of opposite charge to the kaon candidate, assumed to be the slow pion. The number of  $D^{*\pm}$  decays in the sample is estimated from the distribution of  $\Delta m = m_{K\pi\pi_s} - m_{K\pi}$ . The mass difference distribution from H1 is shown in Figure 2, and a clear signal can be seen with a relatively small background.

Kinematic cuts are applied to the  $D^*$  candidates, to ensure clean reconstruction and reduce

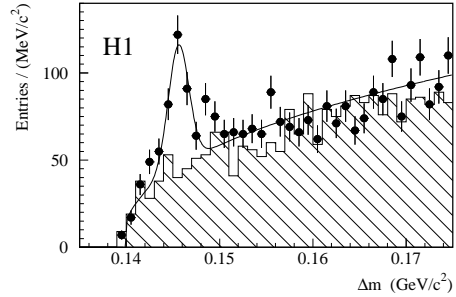


Figure 2. Distribution of  $\Delta m$  for  $D^*$  candidates in photoproduction, as measured by H1.

background. Both experiments require their  $D^*$ s to be in the central region of pseudorapidity,  $-1.5 < \eta < 1.0$  ( $40^\circ < \theta < 155^\circ$ ). H1 apply a  $p_t$  cut of 2.5 GeV, while ZEUS apply cuts of 3(4) GeV for  $K\pi\pi_s$  ( $K\pi\pi\pi\pi_s$ ) signals.

Photoproduction event samples with  $Q^2 < 4 \text{ GeV}^2$  and  $W$  in the range 100 to 200 GeV are identified by activity in the main detector, with no scattered positron detected. The average value of  $Q^2$  is around  $0.2 \text{ GeV}^2$ , and the median value  $5 \cdot 10^{-4} \text{ GeV}^2$ . H1 additionally use a tagged sample where the positron is detected in the small angle luminosity detector, giving an average  $Q^2$  of  $10^{-3} \text{ GeV}^2$ .

From the number of reconstructed  $D^*$ s, the experiments measure the visible cross-section for the reaction  $e^+p \longrightarrow D^*X$  within the kinematic cuts applied, by correcting for acceptance and for the combined branching ratio to the decay channels detected. In order to extract the total charm production cross-section, the visible fraction falling within the cuts must be estimated from Monte Carlo. A further correction must be applied for the probability  $p_{c \rightarrow D^{*+}}$  for the charm quark to fragment to a  $D^*$  meson. The Monte Carlo extrapolation to the full  $D^*$  kinematic region is subject to large uncertainties, arising mainly from the choice of structure functions and of the value of  $m_c$  used in the calculations, and this uncertainty is reflected in the cross-

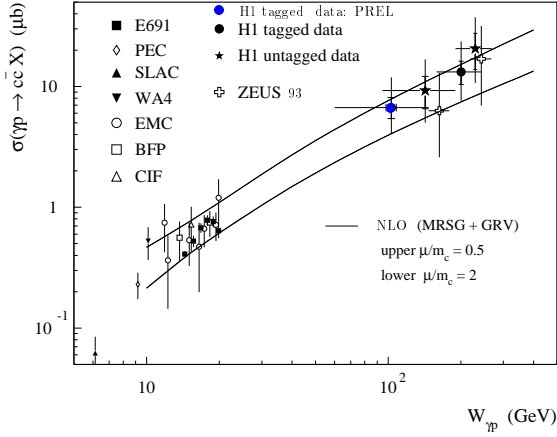


Figure 3. The total cross-section for charm photoproduction, plotted as a function of  $W$ . Error bars include uncertainties due to the model-dependent extrapolation outside the experimental acceptance. Data points from H1 are plotted with inner error bars showing the contribution from statistical and experimental systematic errors only.

section error bars as plotted in Figure 3. The data show an order of magnitude rise in the integrated cross-section relative to lower energy photoproduction measurements, in general agreement with the NLO QCD calculations of [4].

The calculations of differential cross-sections, covering the  $(p_t, \eta, W)$  acceptance of the measurements, are much less sensitive than the total cross-section to the uncertainties mentioned above. When these distributions are plotted, the data are found to lie systematically above the predictions of [4]. The predictions are based on an approach to performing NLO calculations where only light quarks are assumed to be active flavours in the structure functions of the proton and photon. Alternative calculations have been performed[5,6] where charm flavour excitation is allowed to contribute in leading order, giving generally higher predicted cross-sections. These are due principally to the process  $cg \rightarrow cg$ , where the hard scattering is between a charm quark

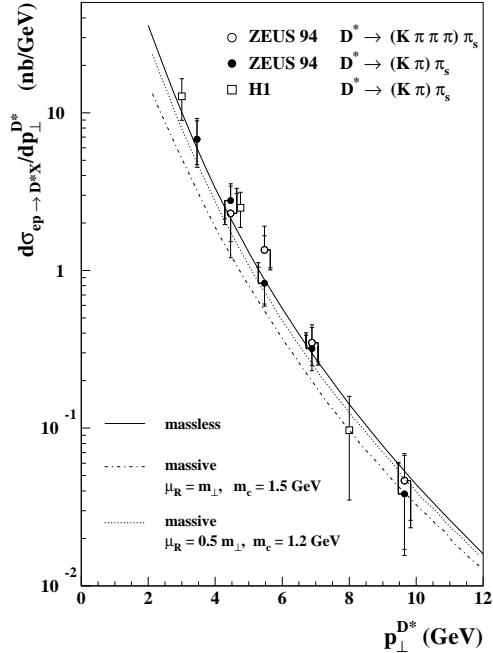


Figure 4. The  $D^* p_t$  spectrum in photoproduction compared with QCD calculations.

from the photon and a gluon from the proton. The two types of calculation are described as massive and massless charm approaches, respectively. Figure 4 shows the measured  $p_t$  spectrum from both experiments, together with the massive charm predictions of [4] using two different values for the charm quark mass  $m_c$ , and the massless charm predictions of [5]. The massless charm approach is seen to give a better description of the data. The calculations of [6], not plotted in Figure 4, are based on a different treatment of the heavy quark fragmentation and also agree well.

### 3. OPEN CHARM IN DEEP INELASTIC SCATTERING

Measurements of charm meson production in DIS events have been used by H1[7] and Zeus[8]

to evaluate the charm contribution to the proton structure function  $F_2(x, Q^2)$ . This contribution  $F_2^{c\bar{c}}(x, Q^2)$  is defined by

$$\frac{\partial^2 \sigma^{c\bar{c}}}{\partial x \partial Q^2} = \frac{2\pi\alpha^2}{xQ^4} \left(1 + (1-y)^2\right) F_2^{c\bar{c}}(x, Q^2) \quad (2)$$

where  $\sigma^{c\bar{c}}$  is the total charm production cross-section. Here the contribution due to longitudinally polarised virtual photons, which is expected to be small, has been neglected. The measurements of  $F_2^{c\bar{c}}$  are also discussed in the contribution on structure functions to this conference[9].

The experiments perform their analyses starting from samples selected by the standard cuts for DIS event samples, principally by requiring the detection of an energetic scattered positron. ZEUS use events in the range  $5 < Q^2 < 100 \text{ GeV}^2$  and H1 require  $10 < Q^2 < 100 \text{ GeV}^2$ . The  $D^*$  decay channel (1) is again used as the signal for charm production by both experiments, while H1 have additionally analysed measurements of inclusive  $D^0$  production.

In order to throw light on the underlying production mechanism, the fractional momentum  $x_D$  of the charm mesons in the  $\gamma^*p$  frame is studied. This quantity is defined by H1 as

$$x_D = \frac{|p_D^*|}{|p_p^*|} = 2 \frac{|p_D^*|}{W} \quad (3)$$

where  $p_D^*$  and  $p_p^*$  are the momenta in this frame of the  $D^0$  and the proton, respectively. The distribution is shown in Figure 5. ZEUS present a similar distribution using the momentum of the  $D^*$  instead of the  $D^0$ . If the charm particles are produced via photon-gluon fusion (PGF), a  $c\bar{c}$  pair is recoiling against the proton remnant in the  $\gamma^*p$  frame. In this case the  $x_D$  distribution is expected to peak below  $x_D = 0.5$ , as observed. In the flavour excitation process where the virtual photon interacts with a charm quark from the sea, the distribution is expected to be shifted towards larger values of  $x_D$ . As shown in Figure 5, the data are consistent with expectations from a pure PGF Monte Carlo. The distributions of the observed events in  $p_t^D$ ,  $\eta^D$ ,  $W$  and  $Q^2$  are also found to be in good agreement with predictions.

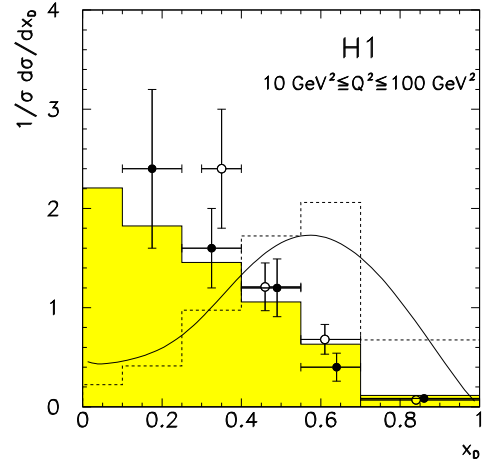


Figure 5. Distribution of  $D^0$  fractional momentum  $x_D$  in DIS measured by H1 (points) compared with expectations from a PGF Monte Carlo (AROMA[10], shaded histogram) and from charm quark sea contributions (dashed histogram and curve).

The measurements of  $F_2^{c\bar{c}}$  are shown in Figure 6, together with results from the EMC[11] fixed target experiment at higher  $x$ . For the low values of  $x$  accessible at HERA,  $x \sim 10^{-3}$ , it is found that  $F_2^{c\bar{c}}$  is around 25% of the total  $F_2$ . Also shown in Figure 6 is the range of predictions from an NLO calculation[12] using the GRV[13] gluon distribution, for charm quark masses between  $1.35 < m_c < 1.7 \text{ GeV}$ . The lowest value of the mass corresponds to the upper boundary of the shaded region in the figure.

The NLO QCD calculation of [12] includes only the PGF diagram as the source of charm production in DIS. This approach is therefore similar to the massive charm calculations for photoproduction discussed in section 2. There it was seen that such an approach gives cross-section predictions which tend to be lower than the photoproduction data, while for DIS the agreement is good within

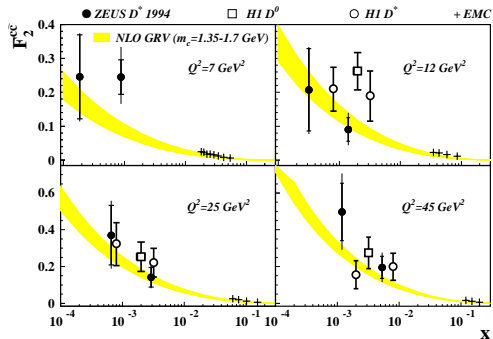


Figure 6. Measurements of  $F_2^{c\bar{c}}$  from 1994 HERA data, plotted as a function of  $x$  in 4 bins of  $Q^2$ . Also shown are fixed target measurements from EMC. The shaded bands are NLO QCD predictions for a range of charm quark masses.

the limited statistical precision of the 1994 data samples.

Again for DIS, there exist alternative treatments within the framework of perturbative QCD, which treat the charm quark as an active parton with its own distribution function  $c(x, Q^2)$ . The charm distribution is driven by evolution from the gluon density, being zero below some threshold  $Q^2$  value of order  $m_c^2$ . These treatments are expected to give improved results for large  $Q^2$  phenomena. A number of authors[14–17] have recently discussed ways to implement such schemes so that the behaviour at  $Q^2 \sim m_c^2$  is essentially given by PGF, to give a description of charm production valid for all scales. Such analyses predict larger values of  $F_2^{c\bar{c}}$  at high  $Q^2$  than expected for pure PGF, a prediction which should be testable with the higher statistics 1995-6 HERA data now being analysed.

#### 4. SUMMARY

Charm production at HERA in real and virtual photon–proton collisions provides an excellent laboratory for detailed tests of perturbative QCD models. This is an area of considerable

experimental and theoretical activity. Models of photoproduction are in reasonable agreement with data at current levels of precision, with some suggestion of the need for a contribution due to “active charm” in the photon. Charm production is found to contribute a substantial fraction of the proton structure function at small  $x$ , as expected given the observed steep rise of the gluon distribution. Precise measurements of  $F_2^{c\bar{c}}(x, Q^2)$  will provide a useful independent constraint on fits to parton distributions, and a check of different approaches to calculations of heavy quark production in perturbative QCD.

#### REFERENCES

1. A. Meyer, these proceedings.
2. H1 collaboration, S. Aid *et al.*, Nucl. Phys. **B472** (1996), 32.
3. ZEUS collaboration, J. Breitweg *et al.*, preprint hep-ex/9704011, accepted by Phys. Lett. **B**.
4. S. Frixione *et al.*, Nucl. Phys. **B454** (1995), 3, and further references therein.
5. B.A. Kniehl *et al.*, Phys. Lett. **B356** (1995), 539.
6. M. Cacciari, M. Greco, Z. Phys. **C69** (1996), 459.
7. H1 collaboration, C. Adloff *et al.*, Z. Phys. **C72** (1996), 593.
8. ZEUS collaboration, J. Breitweg *et al.*, preprint hep-ex/9706009, submitted to Z. Phys. **C**.
9. A. Zhokin, these proceedings.
10. G. Ingelman, J. Rathsman, G.A. Schuler, preprint hep-ph/9605285.
11. EMC collaboration, J.J. Aubert *et al.*, Nucl. Phys. **B213** (1983), 31.
12. B.W. Harris, J. Smith, preprint hep-ph/9706334.
13. M. Glück, E. Reya, A. Vogt, Z. Phys. **C67** (1995), 27.
14. M.A.G. Aivazis *et al.*, Phys. Rev. **D50** (1994), 3102.
15. H.L. Lai, W.K. Tung, Z. Phys. **C74** (1997), 463.
16. A.D. Martin *et al.*, preprint hep-ph/9612449.
17. M. Buza *et al.*, preprint hep-ph/9612398.